Dynamic interchange between $[FeO_4/Na]^0$ configurations in α-quartz

J. Minge,* M. J. Mombourquette, and J. A. Weil
Department of Chemistry, University of Saskatchewan, Saskatoon, Saskatchewan, Canada S7N 0W0
(Received 9 March 1989)

A temperature-dependent reversible change in local symmetry, as well as substantial line broadening, has been observed in the X-band electron-paramagnetic-resonance spectrum of the center $[FeO_4/Na]^0$ in α-quartz in the range 40–70 K. Models for this effect, involving sodium ion hopping across a twofold-symmetry axis of the crystal, are discussed qualitatively. Line-shape analysis yields an Arrhenius activation energy of 39(1) meV and preexponential factor of $1.3(1)\times10^{-12}$ s, consistent with values in the literature obtained from Debye analysis of dielectric relaxation effects.

INTRODUCTION

Six trivalent iron centers, known to exist as impurities in α-quartz, have recently been systematically investigated by us and co-workers by means of the electron-paramagnetic-resonance (EPR) and electron-nuclear-double-resonance (ENDOR) techniques. The species are as follows: electrically-uncompensated center $[FeO_4]^-$,[1] and five cation-compensated centers designated as $[FeO_4/H]^0_{\alpha,\beta}$,[2,3] $[FeO_4/Li]^0_{\alpha,\beta}$,[3,4] and $[FeO_4/Na]^0$.[5] The Fe^{3+} ion in all of these is considered by us to occur substitutionally at a $[SiO_4]^0$ unit in the host crystal, although we note that a controversy around the site assignment of the uncompensated center still exists.[1] The magnetic properties of the compensated $Fe^{3+}(^6S)$ centers appear to be strongly influenced by the nature of the compensating ion. The latter affects not only the magnitude of the spin-Hamiltonian parameters used to describe the EPR spectra of these centers but, what is perhaps most striking, seems to determine each center's effective local symmetry. The $[SiO_4]^0$ units in α-quartz are slightly distorted "tetrahedra," each having its Si atom located (time average) on one of the three polar twofold symmetry axes. The C_2 symmetry is preserved in centers $[FeO_4]^-$ and $[FeO_4/Li]^0_\alpha$ (at least on the X-band EPR time scale and at temperatures above 4 K), but is reduced to C_1 in the other cases. Our recent thermal EPR (X-band) study revealed that the $[FeO_4/Na]^0$ center is unique among the others, in that it shows a reversible conversion from low-temperature C_1 symmetry to effective high-temperature C_2 symmetry, at around 50.5 K. The results of a detailed EPR (X-band) spin-Hamiltonian study of the $[FeO_4/Na]^0$ center at temperature $\approx$20 K will be reported elsewhere.[5] Herein, we will concentrate our attention on the dynamic interchange effect alone, performing a line-shape analysis of spectra in the temperature range 40–70 K.

EXPERIMENTAL

The original yellow-brown iron-doped ($\approx$50 ppm Fe/Si) crystalline α-quartz produced by Sawyer Research Products (Lakeland, Ohio) was electrodiffused with sodium ions at Oklahoma State University. The diffusion was carried out for 8 h at $\approx$490° C in vacuum with an applied electric field of $\approx$20 V/cm along the crystal threefold-(screw) symmetry axis $\hat{\mathbf{c}}$. Sodium chloride evaporated on one crystal surface served as a source of sodium ions; gold electrodes were placed on both surfaces. Before the electrodiffusion, the sample displayed on intense EPR spectrum from the center $[FeO_4/Li]^0_\alpha$. Afterwards, the $[FeO_4/Li]^0_\alpha$ and the $[FeO_4/Na]^0_\alpha$ centers were both present, with comparable intensities. Relatively weak EPR signals originating from the other Fe^{3+} centers (i.e., $[FeO_4]^-$ and $[FeO_4/H]^0$) were also observed, both prior to and after electrodiffusion. The lines belonging to the two newly discovered centers,[3] i.e., $[FeO_4/Li]^0_\beta$ and $[FeO_4/H]^0_\beta$, were also present in our sample, along with other weak and yet unidentified lines.

To describe the EPR spectra, the same reference axis system was used as in our earlier papers;[1,2,4] specifically, the orientation of magnetic field vectors $\hat{\mathbf{B}}$ relative to $\hat{\mathbf{c}}$ and to the axes $\hat{\mathbf{a}}_i$ (crystal twofold axes $\perp\hat{\mathbf{c}}$, $i=1,2,3$) was defined using polar angle $\theta=\sphericalangle(\hat{\mathbf{c}},\hat{\mathbf{B}})$ and azimuthal angle $\phi=\sphericalangle(\hat{\mathbf{a}}_1,\hat{\mathbf{p}}=\hat{\mathbf{c}}\otimes\hat{\mathbf{B}}\otimes\hat{\mathbf{c}})$. The sample was mounted in the EPR cavity in such a way that $\hat{\mathbf{a}}_1\perp\hat{\mathbf{B}}$ and $\hat{\mathbf{a}}_1\|\hat{\mathbf{B}}_1$ (linearly-polarized cw microwave magnetic field). The EPR spectra were measured using a low-temperature EPR cavity system[6] and a Varian V4502 spectrometer operating at a fixed frequency of $\approx$9.92 GHz. The sample temperature was kept constant to within $\pm$0.5 K by thermal conduction to the cold end of a Displex helium refrigerator, equipped with a heater, while the whole resonance cavity was evacuated (pressure $\approx$0.001 torr). The temperature was measured and controlled by a chromel-P versus Au (0.07 at. % Fe) thermocouple (calibrated by immersing its tip in liquid N_2 and/or ice-water mixture) attached to the sample, and a temperature controller (Scientific Instruments Inc., Series 5500). Thermal contact was assured by covering the crystal-thermocouple-holder junction with a copper grease (Crycon grease, APD Cryogenics Inc.). The magnetic field B was measured using a proton NMR gaussmeter, with uncertainty of 1×10^{-3} mT.

Due to the space-group symmetry D^6_3 of (right) α-

quartz and the local C_1 symmetry exhibited by the $[FeO_4/Na]^0$ centers at temperatures below 50 K, the $[FeO_4Na]^0$ centers occur in six symmetry-related sites. These sites (geometric configurations) are labeled i or i' ($i=1,2,3$) where sites i and i' are related by operation of twofold crystal symmetry axis $\hat{\mathbf{a}}_i$. In sites i and i', the Fe^{3+} ion sits on, or is very close to, axis $\hat{\mathbf{a}}_i$. When the sample is rotated around the axis $\hat{\mathbf{a}}_1$ (i.e., $\phi=90°$), all EPR lines remain doubly degenerate. Thus only three EPR lines (stemming from sites 1 and 1', 2 and 3', 3 and 2', respectively), having different angular dependences, can be observed for each fine-structure transition. As the temperature is increased, lines (2,3') and (3,2') begin to broaden and then coalesce at ≈ 50.5 K (at X band). The spectrum, including lines (1,1'), continues to broaden with further heating, until no longer detectable. At any given temperature, the observed stage of motionally-averaged line shape depends on the initial (low-temperature) field-position separation between lines (2,3') and (3,2'), for each individual fine-structure transition at each crystal orientation. The whole dynamic process of interconversion between configurations i and i' is reversible with temperature.

The detailed kinetic EPR study for the $[FeO_4/Na]^0$ center was performed at the fixed crystal orientation defined by angles $\theta=3°$ and $\phi=90°$; the fine-structure EPR transitions $3\leftrightarrow 4$ (transitions between the third and the fourth electron-spin states, numbered in order of increasing energy, i.e., transitions between states labeled with $m_S=-\frac{1}{2}$ and $m_S=\frac{1}{2}$ in the high-field limit scheme) were used. At this orientation the three EPR lines, (1,1'), (2,3'), and (3,2') (occurring at magnetic field ≈ 0.1670 T when the frequency is 9.915 GHz), are well separated but still are close enough to make line recording of the set technically convenient.

RESULTS AND DISCUSSION

The temperature evolution of the overall (three-line) line-shape profile is affected by two distinct processes. The first is the dynamic averaging of the (2,3') and (3,2') EPR lines, and the second is line broadening; the latter can be especially clearly observed on the (1,1') line since here the interchange process does not affect the line shape. The line broadening affects the line-shape profile of all sites quite dramatically just after the distinction between the lines (2,3') and (3,2') vanishes (coalescence). Eventually, and in fact already at temperatures near 70 K (and above), all EPR lines from the $[FeO_4/Na]^0$ center were broadened beyond detection. As a result, in contrast to the remaining other (above-mentioned) iron centers, the EPR spectrum of $[FeO_4/Na]^0$ is not observed at room temperature. It is worth noting that in the temperature interval ($\approx$40–70 K) in which the averaging and the line broadening take place, the distance between the position of line (1,1') and the average position of lines (2,3') and (3,2') is nearly temperature independent. Thus the spin-Hamiltonian parameter matrices (see Ref. 1) averaged over the two interchanging symmetry-related sites seem to be almost temperature independent and the vanishing of the $[FeO_4/Na]^0$ EPR spectrum at the high temperatures can be entirely attributed to magnetic relaxation-time (T_2^*) shortening.

The dynamic process takes place in a magnetically dilute quartz crystal, so that it may be considered as an interchange between two distinct configurations of an isolated $[FeO_4/Na]^0$ center occurring at a fixed location in the α-quartz structure. It is then a two-site exchange case of the type designated as nonmutual (i.e., $[FeO_4/Na]^0$ configurations before and after transition are clearly distinguishable) and spin-uncoupled (i.e., the electron-spin orientations of the two configurations are not related to each other), which can be analyzed using expressions derived from the modified Bloch equations.[7,8] In fact, however, we used the formulation coded in a handy and general program DNMR3H (Ref. 9) (based on the density matrix method) originally developed by Binsch,[10] easily adapted to our X-band EPR case. To compare the theoretically calculated band shape (expressed in frequency units) with our EPR line shapes (collected under fixed-frequency conditions), a linear conversion between the frequency ν and the magnetic field B according to formula $\nu=g_{\text{eff}}\beta_e B/h$ was applied, where $g_{\text{eff}}=4.236(4)$ is the effective g value [average of (2,3') and (3,2') lines] and the other symbols have their usual meaning. The validity of this approximate relation, at the fixed crystal orientation and in the magnetic field range used here, was checked by performing exact numerical calculations (involving complete spin-Hamiltonian matrix diagonalization) of the EPR line positions at different frequencies. For line (2,3') the effective g value was found to be 4.245(4) and for line (3,2') it was 4.227(4). The (total) rate parameter for the configuration interchange at a given temperature was derived by visual comparison of the theoretical band shape [i.e., a convolution of the two motionally-averaged lines (2,3') and (3,2')] with the experimental one. At low temperatures (i.e., no motional averaging) the observed EPR line shapes diverge slightly from being Lorentzian [Fig. 1(a)], probably due to unresolved ^{23}Na hyperfine structure. The slightly different (unresolved) ^{23}Na splittings for each EPR line studied presumably also are the reason why lines (2,3') and (3,2') differ slightly in width; the 20-K peak-to-peak first-derivative width ΔB_{pp} is 0.108(4) mT for line (2,3') and 0.096(4) mT for line (3,2'). The two lines also differ slightly in their (integral) intensities. This difference arises mainly from the different EPR transition probability for each center site, due to their different relative orientation with respect to magnetic fields $\hat{\mathbf{B}}$ and $\hat{\mathbf{B}}_1$. Indeed, exact numerical intensity calculations give $I(2,3')=0.53$ and $I(3,2')=0.47$, respectively [where $I(2,3')+I(3,2')=1$]. By simulation of the experimental line shape (for the preceding two lines) at 20 K (i.e., in the absence of interchange), both the line separation $\delta\nu=42.0(1)$ MHz and the effective intensities $I(2,3')=0.515(4)$ and $I(3,2')=0.485(5)$ were determined. For the line-shape simulations, the difference in the relative intensities of lines (2,3') and (3,2') was taken into account, but the same effective width was assumed for them. These parameters were kept constant, throughout the temperature range studied, in the consecutive simulation runs. Thus the total rate parameter k and the values

of the effective transverse relaxation time T_2^* $[=(\pi 3^{1/2}\Delta\nu_{pp})^{-1}$, where $\Delta\nu_{pp}=g_{\text{eff}}\beta_e\Delta B_{pp}/h]$ were the only parameters varied to obtain the best fits between the experimental and the theoretical band shapes. Three sets of experimental and calculated band shapes, which, respectively, represent the slow-kinetic, coalescence, and fast-kinetic temperature regions, are shown in Figs. 1(b)–1(d). The increasing (with temperature) difference between the experimental and calculated band shapes observed on the low-field side of Figs. 1(c) and 1(d) arises due to increasing overlap (as T_2^* shortens) with the nearby line (1,1'). The values of the obtained average lifetime $\tau=k^{-1}$ and of T_2^*, in the temperature region studied, are listed in Table I.

To interpret the observed data, use was made of the Arrhenius theory for activation processes occurring under thermal equilibrium conditions. The theory, applied to our case, assumes that the (equal) energies of the two distinct center configurations are separated by a temperature-independent potential-energy barrier and that the average lifetime is of the form $\tau=\tau^{(0)}\exp[E_A/(k_BT)]$, where E_A is the activation energy per center, k_B is the Boltzmann's constant, and $1/\tau^{(0)}$ is the so-called frequency factor. To evaluate the parameters, the logarithm of τ versus $1/T$ was plotted, as shown in Fig. 2. It is seen that in the relevant temperature interval, 40–70 K, the experimental data can be well fitted to a straight line with the slope giving activation energy $E_A=39(1)$ meV and the intercept giving $\tau^{(0)}=1.1(1)\times10^{-12}$ s. As depicted in Fig. 2, the values of τ in the fast-kinetic region (above 54 K) are not well determined due to the considerable line broadening. To record any EPR signal at all in this region, fairly extreme experimental conditions were required, i.e., high magnetic-field modulation, high microwave power, and high gain; nevertheless, the signal-to-noise ratio remained quite low (≈4). However, the main reason for rather big uncertainties of τ in the fast-kinetic region is that τ and T_2^* are covariant and cannot be simultaneously well determined from the band-shape analysis of the equally populated two-site system.[11]

The relaxation time T_2^* was found to decrease exponentially with increasing temperature, in the motional-averaging temperature region. The $\ln(T_2^*)$ versus $1/T$ plot included in Fig. 2 indicates that the temperature dependence of T_2^* can also be described as an activation process, with approximately the same activation energy as for the primary kinetic process itself. Fitting of the six high-temperature data points for T_2^* (to the Arrhenius type formula with T_2^* instead of τ) gave the activation energy of 32(1) meV and the preexponential factor of $1.3(2)\times10^{-11}$ s.

To demonstrate that the foregoing results are general (not restricted to our specified experimental conditions) we repeated the (X-band) experiment and the subsequent band-shape analysis for fine-structure lines 3↔4 observed at a different crystal orientation, i.e., at $\theta=31.62°$ and $\phi=90°$. (We were not able to collect enough data over

TABLE I. Temperature dependence of the average lifetime τ and of the effective transverse relaxation time T_2^* for the two $[FeO_4/Na]^0$ centers related by the twofold-symmetry axis bearing the Fe^{3+} ion.

T (K)	$10^8\tau$ (s)	$10^8T_2^*$ (s)
22.2(5)	> 100.0	3.1(3)
38.4(5)	47.0(1.0)	3.1(3)
43.4(5)	3.9(4)	3.1(3)
45.4(5)	2.6(4)	3.1(3)
46.6(5)	2.0(2)	3.3(2)
49.0(5)	1.3(1)	2.20(15)
51.7(5)	0.74(50)	1.70(5)
54.6(5)	0.45(20)	1.20(15)
57.5(5)	0.31(30)	0.80(10)
59.5(5)	0.23(22)	0.60(10)
62.6(5)	0.17(16)	0.45(5)

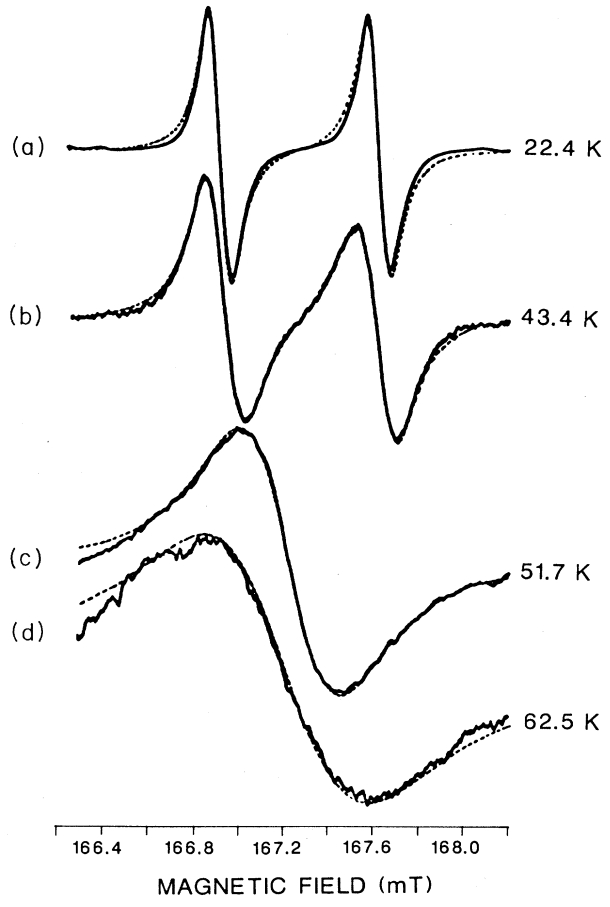

FIG. 1. The experimental (solid curve) and the theoretical (dashed curve) band shapes, calculated using the τ and T_2^* values listed in Table I, for temperature regions labeled, respectively: (a) no motional averaging ($T\ll T_c$ such that no kinetic effects on the EPR line shapes are observable), (b) slow kinetic ($T<T_c$ such that kinetic effects on the line shape are observable), (c) coalescence (when EPR is observed at ≈9.92 GHz, occurs at $T_c\sim51$ K), (d) fast-kinetic ($T>T_c$).

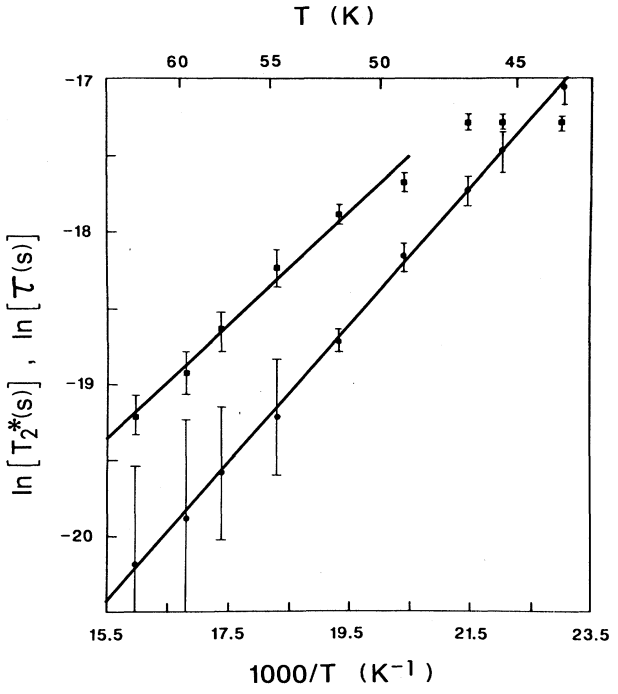

FIG. 2. A semilogarithmic plot of the average lifetime τ (lower) and of the effective transverse relation time T_2^* (upper) vs inverse temperature, for the two $[FeO_4/Na]^0$ configurations related by a twofold-symmetry axis.

the required temperature region to obtain E_A and $\tau^{(0)}$ from other fine-structure lines). In this case the activation energy and the preexponential factor were found 37(1) meV and $9.8(1.0)\times10^{-13}$ s for τ, and 31(1) meV and $9.7(1)\times10^{-12}$ s for T_2^*, respectively. Moreover, the line-shape analysis performed on the (1,1′) line (not affected by the interchanging process) gave an activation energy of 28(1) meV and preexponential factor of $1.8(2)\times10^{-11}$ s for the T_2^* alone.

Three tentative, progressively more elaborate, models to interpret the dynamic interchange between the two symmetry-related sites of $[FeO_4/Na]^0$ will be considered. They are all based on a $[SiO_4]^0$ structural unit containing Fe^{3+} substituted for Si^{4+} and a compensation Na^+ ion located nearby in either of two off-axis positions related by the "original" twofold-symmetry axis. We cannot yet specify the Na^+ position as being on one or the other side of the center (i.e., near the "short" or "long" bonded pair of oxygen atoms; see Ref. 12). It is assumed in all three models that the sodium ion jumps between the two off-axis positions so that in the fast-kinetic region, the Na^+ ion is effectively located on the twofold axis and the original C_2 symmetry of the Si^{4+} (Fe^{3+}) site in the α-quartz structure, disturbed by the presence of the compensating ion, is effectively restored. Since the observed ^{23}Na hyperfine splittings (ENDOR measurements are under way) are close to negligible, we can safely state that the Na^+ ion carries only a very small spin density. Thus the sodium jumps can be considered not to cause direct changes of local magnetic field at the iron ion. Moreover, the magnetic field generated at the Fe^{3+} site by electric charge $|e|$ of the sodium ion moving (oscillating) between the two symmetry-related sites too turns out to be negligible (see Appendix); thus it does not provide a mechanism for the observed high-temperature line broadening.

In the first and crudest model, the sodium ion is considered merely to be a compensating electric charge. As such it affects the properties (thus also the EPR spectra) of the $[FeO_4/Na]^0$ center mainly by generating an important contribution to the electric field at the Fe^{3+} ion. Thus, when the Na^+ ion jumps, there is a change in direction of the resultant electric field gradient and consequently a change in the principal directions of the spin-Hamiltonian parameters (e.g., matrix **D**). In the second model, the sodium ion is considered in addition to participate in the molecular bonding scheme of the $[FeO_4/Na]^0$ cluster and thus via the electron charge (and spin-density) distribution influences the equilibrium positions of all nuclei in the cluster. Accordingly, the sodium ion jumps between the above-mentioned positions are followed by relaxation of the other nuclei (i.e., adjustment of their positions). In the third model, a possibly appreciable electron-spin distribution between the central iron ion and its oxygen ligands is additionally considered, the jump resulting in transfer of hole character from one to another of the oxygens. Here the ground state of the center may be crudely considered to be a mixture of resonance forms of the type $Fe^{3+}O^{2-}$ and $Fe^{2+}O^-$. Thus in this model, the sodium ion jumps between oxygen ions are linked to simultaneous hole jumps between the other pair of symmetry-related oxygens. This can possibly constitute an additional fast magnetic relaxation mechanism dominating T_2^* at higher (>50 K) temperatures. Such a phenomenon is well known in quartz in the center $[AlO_4]^0$.[12]

Another conceivable model for the broadening and disappearance of the EPR signal is to invoke a local high-spin $\rightleftharpoons$ low-spin transition at the Fe^{3+} ion. Presumably this would be, using labels appropriate for tetrahedral symmetry, between states $^6A_1$ and $^2T_2$. It may be that the relatively larger size of the Na^+ ion, as compared to Li^+ and H^+, is relevant in causing distortion, allowing such a strain-sensitive transition to occur.

At present, in the absence of elaborate calculations, we cannot assert which (if any) of these models provides the best description of the actual process. However, the results of *ab initio* Hartree-Fock self-consistent-field (SCF) molecular orbital (MO) calculations done on analogous model clusters, with Al as a central atom instead of Fe,[13] suggest that sodium ion jumping is in fact accompanied by subsidiary electron density transport and nuclear displacements in the whole cluster. The calculations show that the compensating ion in the diamagnetic center $[AlO_4/M]^0$ (as well as in the paramagnetic center $[AlO_4/M]^+$, where M=H,Li,Na) accepts appreciable electron density and participates in the covalent bonding scheme of the cluster. Specifically, in the case of sodium-compensated aluminum centers, it was shown that the sodium ion indeed takes an off-axis position, while being approximately equidistant from two

symmetry-related oxygen atoms of the cluster, and that all atoms of the cluster relax to accommodate the sodium ion at either of its two symmetry-related positions. It was found {while keeping fixed all atom (relaxed) positions in the $[AlO_4/Na]^0$ cluster, except for Na} that the Na ion, on its trajectory across the original twofold-symmetry axis to the other position, is moving in a double-minimum unsymmetrical energy potential well. The estimated (from SCF MO calculations) energy barrier from the deeper minimum in the case of the $[AlO_4/Na]^0$ cluster is 10 meV,[13] which is of the same order of magnitude as the activation energy [39(1) meV] for the interchange of $[FeO_4/Na]^0$ configurations found here.

Recent dielectric relaxation studies (at experimental frequency 1 kHz) in Na-swept synthetic α-quartz doped with iron[14] revealed the presence of two dielectric-loss peaks, at 20 K and 138 K, respectively, related to the presence of the sodium ions. Furthermore, the comparative EPR study reported in Ref. 14 showed that occurrence of the loss peaks correlates with the presence of the observed EPR spectrum, arising from center $[FeO_4/Na]^0$. The peaks, which are close to being of the Debye type, can be described using a single dielectric relaxation time τ_D obeying the relation

$$\tau_D = \tau_D^{(0)} \exp[E_D/(k_B T)] ,$$

with preexponential factor $\tau_D^{(0)}$ and activation energy E_D. For the dielectric-loss peak observed at 20 K, E_D is 30 meV and $\tau_D^{(0)}$ is 6.7×10^{-12} s, which, respectively, are close to the activation energy and the factor $\tau^{(0)}$ derived here from the EPR data of interchanging $[FeO_4/Na]^0$ centers. For a given defect center, such dielectric relaxation responses depend on the existence of a net electric dipole moment and of (at least) two interconvertible configurations for the species; however, no unpaired electrons are required. Our several models are compatible with the observed relaxation results.

The other Fe^{3+} centers known to exist in α-quartz do not exhibit any substantial EPR changes with temperature ($T \leq 300$ K). It is thought that the proton in each center $[FeO_4/H]^0_{\alpha,\beta}$ is bonded to an oxygen ion attached to the ferric ion, and thus does not jump. With Li^+, it may be that jumping occurs in $[FeO_4/Li]^0_\alpha$ already at 4 K, but that it bonds to oxygen in $[FeO_4/Li]^0_\beta$ at low ($\approx$20 K) temperatures.

Similar interchange between two configurations (related by a twofold-symmetry axis) has been observed with the $Ge^{3+}(^2S)$ centers $[GeO_4/Li]^0_C$,[15] $[GeO_4/Na]^0_A$, and $[GeO_4/Na]^0_C$.[16] Center $[GeO_4/Li]^0_A$ retains C_2 symmetry from 4 K upward. No centers of type $[GeO_4/H]^0$ appear to exist. So far, the dynamic interchange effect has been studied in detail only in the case of $[GeO_4/Na]^0_A$, yielding an Arrhenius activation energy of 267(2) meV and a frequency factor of $1.6(1)\times10^{13}$ Hz,[16] both parameters being approximately 1 order of magnitude greater than in the $[FeO_4/Na]^0$ case. Accordingly, the coalescence temperature for the EPR lines stemming from the symmetry-related (C_2) $[GeO_4/Na]^0$ centers is $\approx$230 K at X band. No dramatic line broadening in the fast-kinetic region was observed with Ge, in sharp contrast to our present Fe case. It remains to be seen whether the relationship between Ge centers A and C is similar to that between Fe centers α and β; neither is as yet well understood.

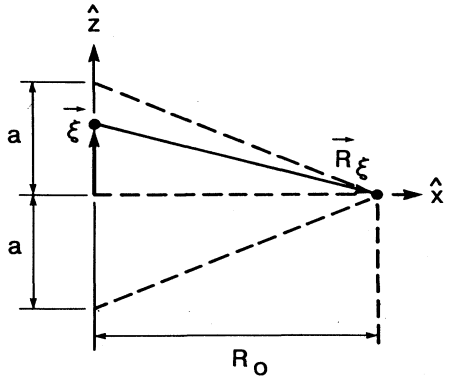

FIG. 3. Auxiliary diagram for calculation of magnetic field **B** produced by a one-dimensional harmonically-oscillating electric charge (see Appendix).

Note added in proof. We have just learned of the appearance of a publication by P. Stegger and G. Lehmann [Phys. Status Solidi B **151**, 463 (1989)] reporting results paralleling our present findings.

ACKNOWLEDGMENTS

The authors wish to thank L. E. Halliburton, A. S. Nowick, J. J. Martin, and B. Sawyer for making the samples available. We wish to thank R. S. Dickson for helpful discussions and technical assistance and D. G. McGavin for useful comments. This work was supported by the Natural Sciences and Engineering Research Council of Canada.

APPENDIX

As a model for the effect at the Fe^{3+} site of the Na^+ jumps, we considered harmonic motion, taking the sodium cation position to be $\xi = a\hat{z}\cos(2\pi\nu t')$, as depicted in Fig. 3. The ferric ion is static at $\mathbf{R}_0 = R_0\hat{x}$. Following the equations [(19) and (1)] given by Janah *et al.*,[17] the electric field and magnetic induction at $\mathbf{R}_0$ an time t are, respectively,

$$\mathbf{E}(R_0,t) = \frac{kq}{c\eta_\xi}\left[\frac{\hat{\mathbf{R}}_\xi}{R_\xi^2} + \frac{d}{dt'}\left[\frac{\hat{\mathbf{R}}_\xi - \mathbf{v}_\xi/c}{\eta_\xi R_\xi}\right]\right]$$

and

$$\mathbf{B} = \hat{\mathbf{R}}_\xi \otimes \mathbf{E}/c ,$$

in SI units [with $k = (4\pi\epsilon_0)^{-1}$, where ϵ_0 is the permittivity of free space]. Here

$$\hat{\mathbf{R}}_\xi = R_\xi \hat{\mathbf{R}}_\xi = \mathbf{R}_0 - \xi$$

is the vector from the Na^+ ion to the Fe^{3+} ion (at time t'), while

$$\mathbf{v}_\xi = \frac{d\xi}{dt'} \quad \text{and} \quad \eta_\xi = 1 - \mathbf{v}_\xi \cdot \hat{\mathbf{R}}_\xi / c \ ,$$

and q is the charge of the Na^+ ion. Light requires time interval $t - t' = R_\xi(t')/c$ to travel from the charge to the field point $\mathbf{R}_0$.

If $v_\xi \ll c$, the magnetic field can be shown to be given by

$$\mathbf{B} = -\frac{1}{2}\mu_0 q \nu \frac{aR_0 \sin(2\pi\nu t')}{[R_0^2 + a^2\cos^2(2\pi\nu t')]^{3/2}}\hat{\mathbf{y}} \ ,$$

where μ_0 is the permeability of free space. With the values $q = |e| = 1.6\times10^{-19}$ C, $\nu = 1.0\times10^{8}$ s^{-1}, $a = 5.3\times10^{-11}$ m, and $R_0 = 2.0\times10^{-10}$ m, one finds the maximum amplitude of the magnetic induction to be $B = 1.3\times10^{-8}$ T.

---

*On leave from Institute of Molecular Physics, Polish Academy of Sciences, Poznań, Poland.

[1]M. J. Mombourquette, W. C. Tennant, and J. A. Weil, J. Chem. Phys. **85**, 68 (1986).

[2]M. J. Mombourquette, J. Minge, M. R. Hantehzadeh, J. A. Weil, and L. E. Halliburton, Phys. Rev. B **39**, 4004 (1989).

[3]J. Minge, J. A. Weil, and D. G. McGavin, Phys. Rev. B (to be published). This paper will report the discovery of a second type (labeled β) of cation (H^+,Li^+)-compensated Fe^{3+} center.

[4]L. E. Halliburton, M. R. Hantehzadeh, J. Minge, M. J. Mombourquette, and J. A. Weil, Phys. Rev. B **40**, 2076 (1989).

[5]M. J. Mombourquette, J. Minge, M. R. Hantehzadeh, J. A. Weil, and L. E. Halliburton (unpublished). It is not yet clear whether a second type of sodium center (i.e., $[FeO_4/Na]^0_\beta$) exists.

[6]B. D. Perlson and J. A. Weil, Rev. Sci. Instrum. **46**, 874 (1975).

[7]H. S. Gutowsky and C. H. Holm, J. Chem. Phys. **25**, 1228 (1956).

[8]M. T. Rogers and J. C. Woodbrey, J. Phys. Chem. **66**, 540 (1962).

[9]W. Stempfle, J. Klein, and E. G. Hoffmann, Quantum Chemistry Program Exchange, No. 450, Dept. of Chemistry, Indiana University, Bloomington, IN 1982.

[10]G. Binsch, J. Am. Chem. Soc. **91**, 1304 (1969).

[11]J. Sandström, *Dynamic NMR Spectroscopy* (Academic, New York, 1982), p. 88.

[12]J. A. Weil, Phys. Chem. Miner. **10**, 149 (1984), and references therein.

[13]M. J. Mombourquette and J. A. Weil, Can. J. Phys. **63**, 1282 (1985).

[14]S. Keilson, S. Ling, A. S. Nowick, and L. E. Halliburton, *Proceedings of the 41st Annual Frequency Control Symposium, Philadelphia, 1987* (Systematics General Corp., Arlington, VA, 1987), p. 223.

[15]J. Isoya and J. A. Weil (unpublished). Also see Y. Haven, A. Kats, and J. S. van Wieringen, Res. Rep. **21**, 446 (1966).

[16]R. S. Dickson (private communication).

[17]A. R. Janah, T. Radmanabhan, and T. P. Singh, Am. J. Phys. **56**, 1036 (1988).